第35卷 第2期 焊 接 学 报 Vol. 35 No. 2
2014年2月 TRANSACTIONS OF THE CHINA WELDING INSTITUTION February 2014

Cu/Ti 异种金属搅拌摩擦焊搭接接头组织与性能

姚 磊[1]， 沈以赴[1]， 李 博[1*]， 胡伟叶[2]
(1. 南京航空航天大学 材料科学与技术学院，南京 210016;
2. 中国航天科工集团 南京晨光厂工艺研究所，南京 210012)

摘 要: 文中采用搅拌摩擦焊法搭接 T2 工业紫铜和 TA2 纯钛，研究了搭接接头的宏观形貌和微观组织结构，并测试了接头力学性能. 结果表明，当选用搅拌头旋转频率为 800 r/min，焊接速度为 40 mm/min 的工艺参数配比时，可以获得焊缝表面成形良好，连接界面无缺陷的搭接接头. 在焊核区，钛和铜以相间的条带结构形式相互混合、紧密连接在一起，形成了涡流状的钛铜双相金属混合区域，而且某些区域呈现出“机械互锁”的组织形貌. 钛铜搭接接头抗剪切力可达到铜母材失效载荷的 95%，断裂位置位于搭接接头铜板前进侧，为典型的韧性断裂.

关键词: 搅拌摩擦焊; 搭接; 钛; 铜; 条带结构
中图分类号: TG453 文献标识码: A 文章编号: 0253-360X(2014)02-0109-04

0 序 言

钛合金作为重要的工程结构材料，因为具有较高的比强度和非常出色的抗腐蚀性能而广泛应用于航空航天、化工、造船、能源等领域. 铜合金作为良好的导电导热材料在上述领域也被广泛应用. 将钛合金和铜合金连接形成复合结构材料具有更加广阔的应用前景. Kemal 等人[1] 对 Ti-6Al-4V 和铜合金进行了扩散连接，研究结果表明在钛铜连接界面处形成了钛铜固溶体复相组织. Meshram 等人[2] 对 CP-Ti 和紫铜进行了摩擦焊接，发现焊接时间过长将会导致金属间化合物中间层的形成，从而导致接头强度降低. Nizamettin 等人[3] 利用爆炸焊进行 Ti-6Al-4V 板材和紫铜板材的连接，在焊缝处没有发现金属间化合物的生成，接头强度非常高. 然而，扩散焊和摩擦焊等连接方式对于工件尺寸存在特殊的要求，这无疑会限制它们的应用[4].

搅拌摩擦焊(FSW)是英国焊接研究所在 1991 年发明的一种新式固态连接方法. 它在铝、铜、钛等金属连接方面取得了非常出色的表现[5-7]，但是目前国内外关于钛铜异种金属的搅拌摩擦焊研究还没有. 因此文中采用搅拌摩擦焊方法对工业纯钛 TA2 和 T2 紫铜异种金属进行了搭接连接试验，研究了接头的界面特征和微观组织以及力学性能，为进一步改进工艺、获得优质焊接接头，促进钛铜异种金属搅拌摩擦焊的应用奠定基础.

1 试验方法

试验母材选用厚度为 2 mm 的 TA2 工业纯钛和 T2 态工业紫铜，其化学成分如表 1、表 2. 焊前板材用砂纸打磨除去氧化膜，并用酒精清洗、烘干. 试验选用组装式搅拌头，如图 1 所示，轴肩采用镍基高温合金制成，直径为 15 mm，搅拌针选用以 WC-Co 为原料的硬质合金制作，直径为 6 mm. 焊接时钛和铜装配的相对位置如图 2 所示. 在大量预试验的基础上，选取搅拌头旋转频率为 800 r/min、焊接速度为 40 mm/min 的工艺参数配比. 焊后沿垂直于焊缝切割试样，制取焊缝接头金相试样. 钛一侧选用 HF: HNO_3: H_2O = 1:2:47 的“kroll”试剂腐蚀，铜一侧用 $FeCl_3$(3.5g) + HCl(25 mL) + 蒸馏水(75 mm) 制成的溶液腐蚀. 在光学显微镜上观察焊缝横截面宏观形貌和接头金相组织，采用扫描电镜观察搭接界面区的微观组织结构，并用能谱仪分析接头的元素分布和含量. 用 SANS 电子万能试验机测试搭接接头的抗剪切力，尺寸选用宽为 15 mm 的矩形剪切试样. 剪切速度为 1 mm/min，工作环境在室温下.

表 1 TA2 工业纯钛化学成分(质量分数，%)
Table 1 Chemical compositions of TA2 titanium

Fe	C	N	H	O	Ti
0.30	0.10	0.05	0.01	0.25	余量

收稿日期: 2012-11-06
* 参加此研究工作的还有周冠男、吴小伟

表2 T2紫铜化学成分(质量分数,%)

Table 2 Chemical compositions of T2 copper

Cu + Ag	Bi	Zn	As	Fe	Pb
99.90	0.001	0.002	0.002	0.005	0.005

图1 试验中所用组装式搅拌头

Fig. 1 Compositional welding tool

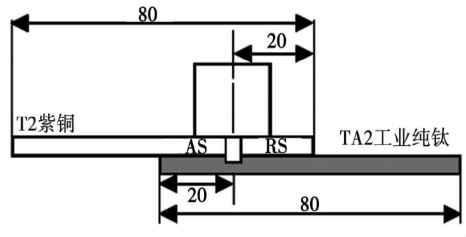

图2 搭接接头原理示意图(mm)

Fig. 2 Schematic diagram of lap joint

2 结果与分析

2.1 搭接接头表面及横截面形貌

图3a为800 r/min,40 mm/min焊接工艺参数下钛铜搅拌摩擦搭焊接头横截面宏观形貌,由图3可知,在所选的工艺参数下,搭接横截面焊接情况良好,无沟槽和裂纹等缺陷. 在搭接接头横截面中间部位,钛与铜成了一个较大范围的混合层区(Mixture Layer),此区域为核心区域,直接决定着Cu/Ti异种金属搅拌摩擦焊搭接接头焊缝成形及力学性能,因此着重对其进行观察分析. 在焊核区,钛侧部分材料从后退侧被搅拌针挤压出来,进入铜一侧,或呈大小不一、形状不规则的长条状(图3b中的Ⅰ区),或呈参差不齐、有大有小的颗粒状(图3b中的Ⅱ区). 将图3b中的Ⅰ区、Ⅱ区在高倍显微镜下观察,分别见图3c,图3d. 从图3c可以看出,钛和铜以相间的条带结构形式相互混合、紧密连接在一起,形成了涡流状的钛铜双相金属混合区域. 从图3d可以观察到,钛侧材料以块状形式与铜侧材料混合在一起,并且分布着一些小块钛颗粒,而且有些区域呈现出“机械互锁”的形貌,Fazel-Najafabadi等人[8]在304不锈钢和CP-Ti的搅拌摩擦搭焊中也发现了这种现象.

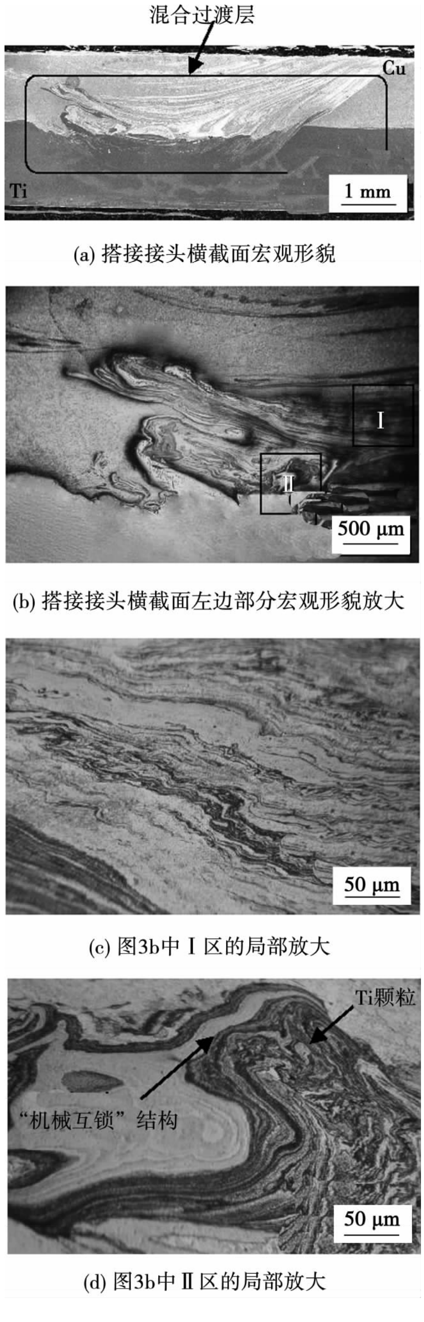

图3 搭接接头宏观形貌

Fig. 3 Macrostructure of Cu/Ti lap interface

分析认为,在焊接过程中,因为搅拌针贯穿整个铜板,加之铜板处于搅拌轴肩下方的“轴肩影响区”范围内,因此铜侧材料塑性变形非常严重,呈现出塑性流动状态. 对于钛侧材料来说,因为搅拌针只是部分的扎入,因此在搅拌针的“搅拌 - 挤压”复合机械作用下,焊核区搭接界面范围内的部分钛金属发生塑性变形,形成长条状或者颗粒状,在搅拌针的摩

擦力和压力共同作用下,这些长条状、颗粒状的钛金属向上运动,进入处于塑性流动状态的铜一侧,与铜侧材料相互混合,形成"机械咬合"式的复相条带状形貌结构. 对于"机械互锁"形貌的形成,是因为在焊接过程中,搅拌头及搅拌针的转动过程和搅拌头焊接行走过程是同时进行的,伴随着垂直面上钛铜金属材料之间塑性材料的相互流动,会导致部分区域形成"机械互锁"的形貌特征.

2.2　搭接界面区微观结构及元素含量

使用扫描电镜和能谱分析仪对搭接界面中心部位的微观结构和成分进一步分析,如图 4 所示. 从图 4a 可以看出,Cu/Ti 搅拌摩擦焊搭接接头的搭接界面局部区域呈涡流状钛铜相间的条带组织结构形貌,此处区域条带状组织结构混合较为充分,浅灰色区域中的黑点为腐蚀微孔.

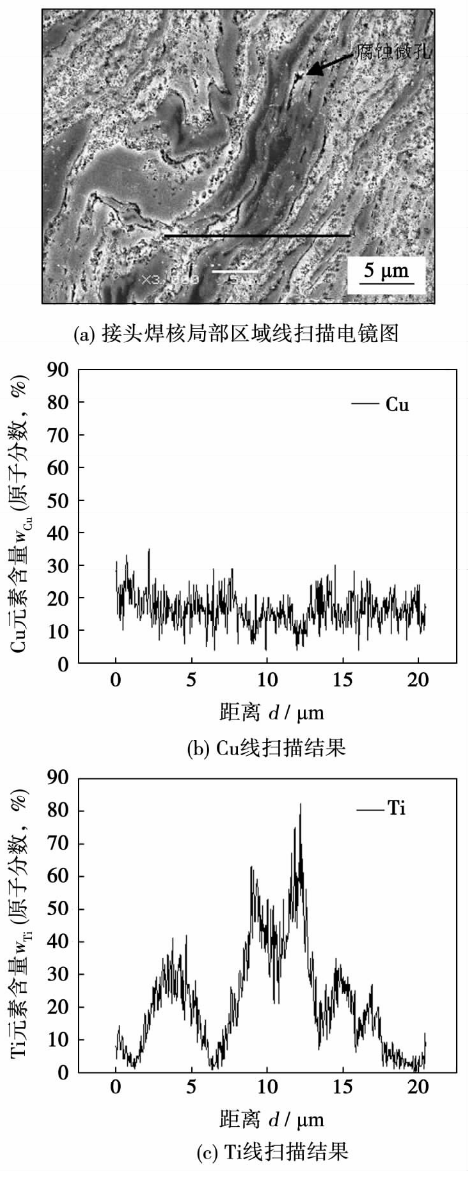

图 4　Cu/Ti 搭接接头线扫描电镜图

Fig. 4　Qualitative EDS line analysis of Cu/Ti lap interface

对图 4a 中正下方区域进行线扫描电镜能谱分析(图中所示黑色线条),结果如图 4b,c 所示. 从图 4b,c 中可以看出,沿扫描线从左到右,钛和铜峰值交替升高降低,说明钛与铜在此处区域是以混合形式存在,而且从线扫结果可以看出,此线扫描区域还存在除 Ti,Cu 以外的其它元素.

2.3　接头力学性能、断口的 SEM 及分析

图 5 为 Cu/Ti 搭接接头断裂位置和断口扫描电镜图. 在旋转频率为 800 r/min、焊接速度为 40 mm/min的焊接工艺参数配比下,钛铜搭接接头抗剪切力为 8.40 kN,略小于铜母材的抗拉失效载荷(8.85 kN),达到铜母材抗拉失效载荷的95%. 搭接接头抗剪强度较高,分析原因,首先是因为焊核区内的铜板母材和钛板上层部分母材在搅拌针的搅拌和行走过程中受到了充分的机械混合,形成条带状形貌机械混合区域;其次在焊接过程中,焊核区发生动

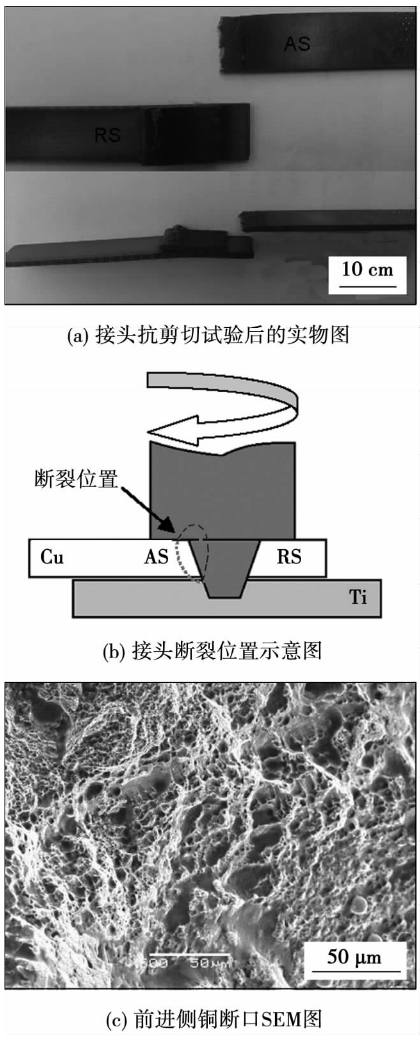

图 5　Cu/Ti 搭接接头断裂位置和断口扫描电镜图

Fig. 5　Fracture locations of Cu/Ti joints and SEM image of fractured surface

态再结晶，微观组织晶粒细化，从而导致焊核区细晶强化; 最后钛铜在焊接温度场下会发生互相扩散，形成钛铜有限固溶体，形成固溶强化作用. 在机械均匀混合、细晶强化、固溶强化三方面的作用下，搭接接头抗剪切强度变高.

图5a为Cu/Ti异种金属搭接接头抗剪切试验后的实物图，从图5a中可以看到接头断裂位置位于上层铜板前进侧，断口呈现出典型的45°塑性断裂宏观形貌.

图5b为接头断裂位置示意图，断裂位置位于搭接接头前进侧搅拌针边缘处(图5b)，此处是搅拌区域和热影响区的临界处，在搅拌摩擦焊搭接过程中，此处一般会产生应力集中，在力学试验中成为裂纹产生和扩展的源头，而且在FSW接头中，前进侧为焊接接头的薄弱区[9]，所以此次试验，接头断裂位置也发生于此.

图5c为前进侧铜断口扫描图，可以看出，断口中韧窝较多，且大小不一，断裂形式为韧性断裂.

3 结 论

(1) 采用搅拌摩擦焊，成功的实现了Cu/Ti异种金属搭接焊接. 当选用搅拌头旋转频率为800 r/min，焊接速度为40 mm/min的工艺参数配比时，可以获得焊缝表面成形良好，连接界面无缺陷的搭接接头.

(2) 焊核区，钛和铜以相间的条带结构形式相互混合、紧密连接在一起，形成了涡流状的钛铜双相金属混合区域，而且某些区域呈现出“机械互锁”的组织形貌.

(3) 在旋转频率为800 r/min、焊接速度为40 mm/min的焊接参数配比下，钛铜搭接接头抗剪切力可达到铜母材抗拉失效载荷的95%，断裂位置位于搭接接头铜板前进侧，为韧性断裂.

参考文献:

[1] Kemal A, Yakup K, Nizamettin K. Experimental study of diffusion welding/bonding of titanium to copper [J]. Materials and Design, 2012, 37: 356-368.

[2] Meshram S D, Mohandas T, Madhusudhan Reddy G. Friction welding of dissimilar pure metals [J]. Journal of Materials Processing Technology, 2007, 184: 330-337.

[3] Nizamettin K, Behcet G. Microstructural and mechanical properties of Cu-Ti plates bonded through explosive welding process [J]. Journal of Materials Processing Technology, 2005, 169: 67-71.

[4] Dressler U, Biallas G, Mercado U A. Friction stir welding of titanium alloy TiAl6V4 to aluminium alloy AA2024-T3 [J]. Materials Science and Engineering A, 2009, 526: 113-117.

[5] 刑 丽，柯黎明，刘鸽平，等. 铝合金LD10的搅拌摩擦焊组织及性能分析 [J]. 焊接学报，2002，23(6)：55-58.
Xing Li, Ke Liming, Liu Geping. Microstructure and mechanical properties of a friction stir welded LD10 aluminum [J]. Transactions of the China Welding Institution, 2002, 23(6): 55-58.

[6] Hwang Y M, Fan P L, Lin C H. Experimental study on friction stir welding of copper metals [J]. Journal of Materials Processing Technology, 2010, 210: 1667-1672.

[7] Liu H, Nakata K, Yamamoto N, *et al.* Friction stir welding of pure titanium lap joint [J]. Science and Technology of Welding and Joining, 2010, 15: 428-432.

[8] Fazel-Najafabadi M, Kashani-Bozorg S F, Zarei-Hanzaki A. dissimilar lap joining of 304 stainless steel to CP-Ti employing friction stir welding [J]. Materials and Design, 2011, 32: 1824-1832.

[9] 刘会杰，刘 超，沈俊军，等. 铝-铜的搅拌摩擦焊研究 [J]. 焊接，2009(9)：11-15.
Liu Huijie, Liu Chao, Shen Junjun. The research of aluminum and copper of friction stir welding [J]. Welding & Join, 2009, (9): 11-15.

作者简介: 姚 磊，男，1986年出生，硕士研究生. 主要从事异种金属搅拌摩擦焊研究. Email: yarlead@163.com

通讯作者: 沈以赴，男，教授，博士生导师. Email: yifushen_nuaa@hotmail.com

consumables, and the microstructure of the joints and the tensile strength of weld joints were studied. Results indicate that with the recommended welding parameters, the weld joints possessed high tensile strength with Al-Si welding wires, and the microstructure of the weld was as cast microstructure of dendrite, which was different with the cellular crystal of the fusion zone. The crystalline grain in the HAZ was slightly coarsened by the influence of the welding thermal cycles. The tensile strength and the tendency of forming large pores of the ER4043 weld joint was relatively lower than the ER4047 joint, but the ductility of joint welded with ER4043 was better.

Key words: marine aluminum alloy; TIG; microstructure; mechanical properties

Properties improvement of supersonic plasma spraying Cr_3C_2-NiCr coating by ultrasonic impact treatment

CHEN Jian[1], LV Lin[2], CUI Ting[3], MA Wanbin[1], SHI Hesheng[2] (1. Provicial Laboratory of Advanced Welding Technology, Jiangsu University of Science and Technology, Zhenjiang 212003, China; 2. Nan Jing Run Bang Clad Metal Material Co., Ltd, Nanjing 211803, China; 3. The Changzhou Haojue Suzuki Motorcycle Co., Ltd, Changzhou 213022, China). pp 95 – 98

Abstract: For the ideal resistance characteristics to wear, oxidation and corrosion, Cr_3C_2-NiCr coating has been widely used in the gas erosive wear, abrasive wear, fretting wear and hard surface wear under high temperature conditions. In this paper, Cr_3C_2-NiCr coating on CuCrZr was obtained by supersonic plasma-spraying method, and the post-processing ultrasonic impact treatment was utilized to certain coating. The results show that porosity of the coating decreases from 2.34 percent to 1.83 percent, and average micro-hardness of coating increases from 8.9 GPa to 9.6 GPa and hardness distribution becomes uniform. Coating thermal shock life at 650 ℃ improves markedly; meanwhile, crack path of thermal shock also changes.

Key words: ultrasonic impact treatment; supersonic plasma spraying; Cr_3C_2-NiCr coating; coating properties

Properties of Al-Mg alloys joints welded by refill friction stir spot weldeing process

WANG Lianfeng, ZHU Xiaogang, QIAO Fengbin, GUO Lijie (Shanghai Aerospace Equipments Manufacturer, Shanghai 200245, China). pp 99 – 103

Abstract: In order to determine the properties of refill friction stir spot welded (RFSSW) Al-Mg alloys joints, tests on tensile/shear strength, cross-tension strength, microstructure and fatigue properties of refill friction stir spot welded joints were conducted with 2mm-thickness 5A06 aluminum alloy as research subject, and microstructure model of RFSSW joint was established as well. Experimental results indicated that the microstructure of the joints could be divided into nugget zone, heat affected zone, thermo-mechanically affected zone and base material, respectively. When the rotational speed was 2 000 rpm, the tensile/shear strength was able to reach 8 194 N, and the highest cross-tension strength was 3565N. SEM and OM analysis showed that fatigue cracks initiated from weld edge on the joining surface of the upper and lower plates, and defects including ring groove, cavity, aluminum clad in this area, as well as stress concentration were the main causes for fatigue damage.

Key words: Al-Mg alloy; refill friction stir spot welding; properties

Engineering applications of MIG welding deformation simulation of aluminum alloy sheet

LI Xiaodong, LI Chunguang, ZHU Zhimin, XU Fenglin (CSR Nanjing Puzhen Co., Ltd., Nanjing 210031, China). pp 104 – 108

Abstract: It is a great challenge to control the welding deformation of aluminum alloy sheet because of its characteristics of both material and structure. This kind of deformation is a key problem of welding quality in the railway industry. In this paper, more attentions have paid to welding distortion of joints made of aluminum alloy sheet by MIG welding. Herein, numerical simulation was served as an effective tool for simulating welding deformation. Based on moving heat source model and sectional temperature function, the welding process of top slab of end wall with 2.2mm thickness was simulated. Results showed that range of error between the deformation values of simulation and actual measurement was within 20%, the morphology of the welding pool simulated was basically in agreement with the experimentally measured results. Backward deformation and simulated structure coincide well with the results of actual welding process, welding process optimization of top slab of end wall was carried out by controlling arm pressure and position, welding sequence and backward deformation method.

Key words: aluminum; body sheet; welding deformation; Simulation

Microstructure and properties of dissimilar materials Cu/Ti lapped joint by friction stir welding

YAO Lei[1], SHEN Yifu[1], LI Bo[1], HU Weiye[2] (1. College of Material Science and Technology, Nanjing university of Aeronautics and Astronautics, Nanjing 210016, China; 2. Technology Research Institute of Nanjing Chenguang Group Co., Ltd., China Aerospace Science and Industry Corporation, Nanjing 210012, China). pp 109 – 112

Abstract: The lap joint of commercial purity titanium (TA2) and copper (T2) plates were successfully produced via friction stir welding technique, the macrostructure and microstructure of Cu/Ti lap interface were researched respectively. The mechanical properties of the joint were characterized by tensile shear tests as well. The results show that the defect-free lapwelds with well-formed surface and interface of joint were obtained when rotation speed and travel speed were 800 r/min, 40 mm/min respectively. The interface of joint exhibited the typical bounded texture microstructure of Cu and Ti in the stir zone, and a region of swirling-like of bimetallic weld of TA2 titanium and T2 copper was formed. Moreover, mechanical interlock was formed in some parts of lap joint. A maximum failure load of 95% of the one of T2 copper was achieved, and the fracture location was located in the advancing side of copper, the fracture was the typical ductile fracture.

Key words: friction stir welding; lap; copper; titanium; bounded texture microstructure